High-field magnetization and electron spin resonance in the spin-gap system η-$Na_{1.286}V_2O_5$

A. M. Ghorayeb
Aix-Marseille Université, IM2NP, CNRS UMR 6242, Case 142, Faculté des Sciences de Saint-Jérôme, F-13397 Marseille Cedex 20, France

M. Costes, M. Goiran, and J.-M. Broto
Laboratoire National des Champs Magnétiques Pulsés, CNRS UMR 5147, B.P. 4245, 143 Avenue de Rangueil, F-31432 Toulouse Cedex 4, France

S. Schäfer
Aix-Marseille Université, IM2NP, CNRS UMR 6242, IRPHE, 49 rue Joliot Curie, B.P. 146, Technopôle de Château-Gombert, F-13384 Marseille Cedex 13, France

R. Hayn
Aix-Marseille Université, IM2NP, CNRS UMR 6242, Case 142, Faculté des Sciences de St-Jérôme, F-13397 Marseille Cedex 20, France

J. Richter
Institut für Theoretische Physik, Universität Magdeburg, PF 4120, D-39016 Magdeburg, Germany

P. Millet
Centre d'Elaboration de Matériaux et d'Etudes Structurales, CNRS UPR 8011, B.P. 4347, 29 rue Jeanne Marvig, F-31055 Toulouse Cedex, France

A. Stepanov
Aix-Marseille Université, IM2NP, CNRS UMR 6242, Case 142, Faculté des Sciences de St-Jérôme, Avenue Escadrille Normandie-Niémen, F-13397 Marseille Cedex 20, France

(Received 15 February 2008; revised manuscript received 6 May 2008; published 20 June 2008)

In this work, we report results of high-field magnetization and electron spin resonance (ESR) measurements performed on η-$Na_{1.286}V_2O_5$, a compound that shows a spin gap. This system may be regarded as an assembly of weakly interacting magnetic entities, each of which containing, at low temperature, 18 antiferromagnetically (AF)-coupled $S=\frac{1}{2}$ spins. The purpose of this work is to determine the gap value and to probe the low-lying energy levels in this compound. On the one hand, the high-field magnetization measurements, performed at temperatures down to 1.7 K on powder samples, suggest a spin gap, Δ, of approximately 39 K, a value which is quite close to the earlier estimate of 35 K, which some of us deduced from the susceptibility measurements at low field [Duc *et al.*, Phys. Rev. B **69**, 094102 (2004)]. On the other hand, these measurements show a magnetization step at one ninth of the saturation magnetization, giving strong support to the assumption that this system may be regarded as a finite-size system composed of 18 AF-coupled $S=\frac{1}{2}$ spins. A theoretical fit of the magnetization indicates the necessity to include couplings to second or more distant neighbors. The ESR data at various frequencies (from 9.6–980 GHz) and at temperatures ranging from 4.2–150 K, obtained on powder samples as well as on single crystals, are in accordance with the gap value mentioned above. In addition, these ESR data indicate that the closure of the gap is not accompanied by any detectable mixing between the singlet level and the lowest-lying level of the first excited triplet. This implies the absence of any appreciable Dzyaloshinskii-Moriya interaction in this compound.

DOI: 10.1103/PhysRevB.77.224434 PACS number(s): 76.30.−v, 75.30.Et

I. INTRODUCTION

It is well known that electron spin resonance (ESR) and magnetization measurements performed at high magnetic fields constitute a powerful way to probe the magnetic excitation spectra of solids, particularly in low-dimensional quantum spin systems (see, for example, Refs. 1 and 2).

The system, which we are studying here, is the vanadium oxide bronze η-$Na_{1.286}V_2O_5$, which can also be denoted by the stoichiometric formula $Na_9V_{14}O_{35}$. The room-temperature structure of this compound was reported in 1999 (Refs. 3 and 4) and, recently, its low-temperature structure was published.[5] While the details of the structure may be found in the above references, we shall simply remind the reader here that, owing to a structural second-order phase transition that this compound undergoes at about 100 K, its low-temperature structure differs from that at room temperature mainly by a doubling of the lattice parameter in the ***b*** direction. From the magnetic point of view, the high-temperature phase of this compound may be regarded as being based on magnetic units composed of nine antiferro-

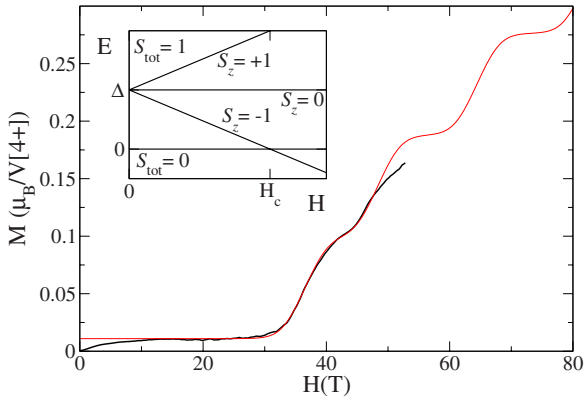

FIG. 1. (Color online) Magnetization curves of η-$Na_{1.286}V_2O_5$ at $T=1.7$ K: experimental curve measured on a powder sample in a magnetic field going up to 52 T (continuous curve) and theoretical fit, up to 80 T, based on a Heisenberg ladder with nearest-neighbor exchange $J\simeq 54$ K and interchain coupling $J_{rung}=1.3$ $J\simeq 70$ K (dashed curve). The inset schematically illustrates the lowest energy states of the system.

magnetically (AF)-coupled $S=\frac{1}{2}$ spins, whereas in the low-temperature phase, owing to the doubling of the lattice parameter, each magnetic unit would contain 18 AF-coupled $S=\frac{1}{2}$ spins. The magnetic susceptibility shows, accordingly, a spin-gap behavior.[4,5]

A tentative estimate of the spin gap in η-$Na_{1.286}V_2O_5$ was first given by Whangbo and Koo[6] who proposed a value of about 183 meV (hence equivalent to 2120 K) deduced from a theoretical calculation based on a spin-dimer analysis. However, our magnetic-susceptibility[5] and X-band ESR measurements[5,7] led us to propose quite a different estimate, whereby the gap, Δ, would only be of the order of 35 K.

Our present study is therefore partially motivated by the need to clarify this issue. Furthermore, an equally interesting motivation is to check whether or not the assumption that this system may be regarded as a finite-size system is reasonable. For this purpose, we have performed high-field magnetization and electron spin resonance measurements. Indeed, a finite-size system with an even number of AF-coupled $S=\frac{1}{2}$ spins would, in zero field, have a singlet ground state followed by a triplet as the first excited state (see the inset in Fig. 1 for an illustration). In the presence of a sufficiently high magnetic field, the Zeeman splitting of the triplet leads to the situation where, above a certain critical field, H_c, the lowest state of the triplet becomes the ground state. The magnitude of H_c solely depends on the spin gap and the g factor, yielding H_c around 27 T for an estimated Δ of 35 K and a g factor as given in Refs. 5 and 7. In the present work, we show that the experimental data are best reproduced for $\Delta\sim 39$ K, which is only slightly higher than the previous estimate. Besides, the magnetization data obtained at 1.7 K indicate a magnetization step occurring at one ninth of the saturation magnetization value. This feature gives strong support to the assumption that this compound may be regarded as a finite-size system, the basic entity of which containing 18 spins. A theoretical fit of the magnetization indicates the necessity to include couplings to second or more distant neighbors. A possible model is that of a 9 $\times 2$ spin ladder, probably with additional frustrating couplings; but the magnetization data alone are not sufficient to determine the exchange couplings uniquely. On the other hand, our ESR measurements performed at different frequencies (at fields below and above the critical value H_c) allow us to suggest that the crossing of the lowest levels at H_c is not accompanied by a mixing of these levels, ruling out therefore the presence of any appreciable Dzyaloshinskii-Moriya interaction in this system.

II. EXPERIMENT

The samples studied in this work were either single crystals or powder samples, prepared following the same procedure as described in Ref. 5 (for the high-field magnetization measurements, only powder samples were studied).

The ESR measurements were performed at various frequencies ($f=9.6$, 96, 344, 738, and 980 GHz). The measurements at $f=9.6$ GHz were conducted on a *Bruker EMX* spectrometer at the Institute of Materials, Microelectronics, and Nanoscience of Provence in Marseille, France. The higher-frequency measurements were performed at the National Laboratory of Pulsed Magnetic Fields in Toulouse, France, in the presence of pulsed magnetic fields going up to 40 T. Microwaves used for these high-field measurements were obtained from a Fabry-Perot cavity optically pumped by a CO_2 laser, in the presence of a gas such as CD_3OD, CH_3OD, or CD_3OH (the choice of the gas depending on the wavelength needed) and were then directed through brass tubes to the sample that was located at the center of a nitrogen-cooled pulsed coil. A field pulse with a duration of 800 ms (rising time of 120 ms) could then be generated by the discharge of a 10-kV capacitor bank on the coil. The radiation transmitted through the sample was detected by an InSb detector cooled to liquid helium temperature.

For the high-field magnetization measurements, pulsed magnetic fields going up to 52 T could be produced, with a pulse duration of 250 ms (rising time of 40 ms). Using a system of two cocentric coils connected in opposition and equipped with additional compensation coils, the derivative of magnetization with respect to time could be monitored and could then be integrated numerically to give the magnetization data.

All of the above measurements were performed as a function of temperature, down to 4.2 K for the ESR measurements and down to 1.7 K for the magnetization.

Whereas only powder samples were used for the magnetization measurements, ESR measurements were performed both on powder samples as well as on single crystals. The X-band study on single crystals was conducted in two configurations of the static magnetic field, H, namely, for H parallel and H perpendicular to the (x,z) plane of the structure (for the definition of the x, y, and z directions, we refer to the notations used in Ref. 5). For the higher-frequency measurements, only the case where H was perpendicular to the (x,z) plane could be studied because, in the other configuration [H parallel to the (x,z) plane], the signal-to-noise ratio was too low to allow reliable data to be obtained.

The g-factor values, $g_{\parallel}=1.973$ and $g_{\perp}=1.931$, as deduced from the room-temperature X-band ESR spectra, are typical

of V^{4+} ions in a fivefold pyramidal environment (see, e.g., Refs. 8 and 9).

III. RESULTS AND DISCUSSION

A. Magnetization: Experiment results

The continuous curve in Fig. 1 shows the experimentally measured magnetization, M, of a powder sample of η-$Na_{1.286}V_2O_5$, at $T=1.7$ K, for magnetic fields in the range of 0–52 T. One may notice from these data that, first, at low fields ($H \lesssim 15$ T), the curve shows the signature of paramagnetic spin-$\frac{1}{2}$ impurities, which rapidly saturate at $M \simeq 0.01\ \mu_B/V^{4+}$. [The presence of such impurities has already been mentioned in earlier magnetic studies (magnetic susceptibility and X-band ESR)[5,7] performed on such samples and in which the concentration of these impurities was found to be very small (~0.005).] Then, at around $H_c \simeq 30$ T, a sudden increase in the magnetization occurs. This value of H_c corresponds to a gap of ~39 K, a value which is not far from the 35 K value which we estimated earlier.[5,7] More interestingly, the experimental curve of Fig. 1 shows a magnetization step occurring at around 43 T and at which the magnetization value is $M \simeq 0.11\ \mu_B/V^{4+}$. Above this step, the curve rises again sharply at higher fields. Based on these experimentally observed results, we may already deduce the following: (i) the zero-field ground state of η-$Na_{1.286}V_2O_5$ is nonmagnetic, apart from spin-$\frac{1}{2}$ impurity contributions not to be considered in the following; (ii) the 9-site spin-$\frac{1}{2}$ magnetic entities—which are the basic building blocks of η-$Na_{1.286}V_2O_5$—must thus be paired up to form a singlet ground state at low magnetic fields; (iii) in agreement with the previous statement, the height of the experimental magnetization step, $M \simeq 0.11\ \mu_B/V^{4+}$, indicates the transition to a triplet ground state since it roughly corresponds to 1/9 of the saturation magnetization when this quantity is expressed per V^{4+} ion. Indeed, taking $g=1.959[=\frac{2}{3}(1.973)+\frac{1}{3}(1.931)]$, the saturation magnetization of an 18-site spin-$\frac{1}{2}$ cluster is given by $M_{sat}=18Sg\mu_B=17.631\mu_B$, so that, when distributed over the 18 magnetic V^{4+} sites, one ninth of the saturation magnetization per V^{4+} ion will have the value $0.1088\ \mu_B/V^{4+}$.

B. Magnetization: Theoretical results

Given these characteristics, the most natural starting point for modeling the experimental magnetization curve is an antiferromagnetic 18-site spin-$\frac{1}{2}$ Heisenberg model, $\hat{H}=\Sigma J_{ij}\mathbf{S}_i\cdot\mathbf{S}_j$. Unfortunately, the simplest model of this type, where the magnetic exchange J_{ij} between spins is restricted to nearest neighbors only, is ruled out because, for an even number of sites, it leads to magnetization curves which are quite different from what is observed experimentally: they start out with a relatively short singlet phase for small applied magnetic fields, followed by a wider first plateau (see continuous line in Fig. 2). The most obvious cure for these shortcomings is to introduce further exchange couplings between more distant neighbors. At this point, however, it should be stressed that the experimental magnetization curve only probes the very small fraction of the $2^{18}=262\ 144$ eigenstates of an 18-site Heisenberg model responsible for low-temperature magnetism, which essentially are given by the lowest-lying $S_z^{tot}=0$, 1 and 2 states. Hence, one anticipates that the experimental data alone are not stringent enough to determine uniquely the parameter set of $J_{ij}s$ prevailing in η-$Na_{1.286}V_2O_5$.

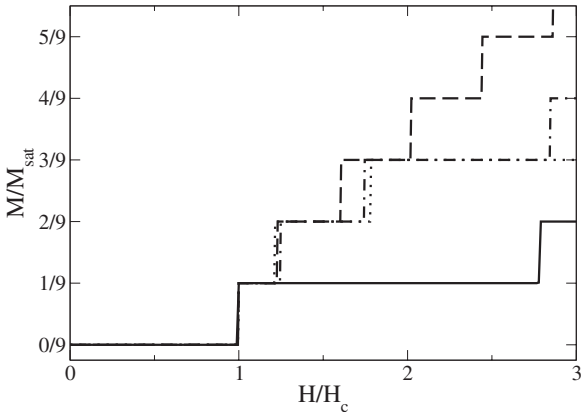

FIG. 2. Magnetization as a function of the applied field (in units of the critical field H_c) for various 18-site Heisenberg clusters; solid line: ring with antiferromagnetic nearest-neighbor coupling J only [model presented in Fig. 3(a)], dashed line: two-legged ladder with antiferromagnetic nearest-neighbor coupling $J_{leg}\equiv J$ and antiferromagnetic interchain coupling $J_{rung}=1.3\ J$ [model presented in Fig. 3(b)], dotted line: ring with antiferromagnetic nearest-neighbor coupling J and antiferromagnetic next-nearest-neighbor coupling $J'=0.6\ J$ [model presented in Fig. 3(c)], and dot-dashed line: two-legged ladder with nearest-neighbor J and next-nearest-neighbor $J'=0.5\ J$ and interchain $J_{rung}=0.6\ J$ [model presented in Fig. 3(d)].

Therefore, we focus in the following on extensions of the nearest-neighbor exchange Heisenberg model, which seem plausible on microscopic grounds, namely (i) a site-by-site coupling between two adjacent 9-site chains resulting in an 18-site ladder [see Fig. 3(b)], and (ii) an antiferromagnetic next-nearest-neighbor exchange between V^{4+} ions via the 180-degree oxygen bond [see Fig. 3(c)] or a combination of both as in Fig. 3(d).

As illustrated in Fig. 2, it turns out that the coupling constants in all these extended models can be tuned in order to

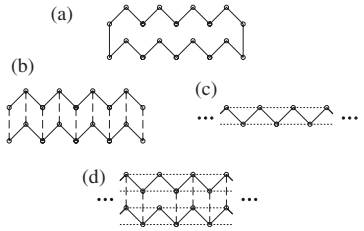

FIG. 3. (a) Plain (nearest-neighbor exchange J) 18-site Heisenberg ring; (b) two 9-site Heisenberg chains, each with a nearest-neighbor exchange constant J, coupled via an interchain coupling J_{rung}, resulting in a two-legged ladder (open boundary conditions); (c) a part of an 18-site Heisenberg ring, with nearest-neighbor exchange J and (frustrating) next-nearest-neighbor exchange J'; (d) an 18-site cluster with interchain coupling J_{rung} and next-nearest-neighbor exchange J' (open boundary conditions).

TABLE I. Optimal fit for the nearest-neighbor exchange coupling J and the proportionality constant α for the models shown in Fig. 3, using $T=1.7$ K as in the experiment. By tuning J' and/or J_{rung} to the values indicated in the text, the models [Figs. 3(b)–3(d)] can be made to reproduce the experimental data almost equally well, while the plain Heisenberg model [Fig. 3(a)] suffers from the deficiencies described in the text. The last two columns summarize, respectively, the paramagnetic Curie temperature θ_C of the model and the temperature for which the susceptibility is maximal (both measured in units of J).

Model	J (K)	α (TV^{4+}/μ_B)	H_{corr} (in T)	θ_C (in J)	χ_{max} at T (in J)
3(a)	192	39.0	≤ 5.9	−0.5	0.64
3(b)	53.9	29.1	≤ 4.3	−0.7694	0.98
3(c)	102	36.0	≤ 5.4	−0.8	0.31
3(d)	81.6	19.3	≤ 2.9	−0.7889	0.45

give the experimentally observed long zeroth ($S^{\text{tot}}=0$) and comparatively short first ($S^{\text{tot}}=1$) plateau. In units of the antiferromagnetic nearest-neighbor exchange coupling J, the appropriate parameters are: $J_{\text{rung}}=1.3$ J for the 18-site ladder shown in Fig. 3(b), $J'=0.6$ J for the next-nearest-neighbor Heisenberg ring shown in Fig. 3(c), and $J'=0.5$ J and $J_{\text{rung}}=0.6$ J for the frustrated ladder shown in Fig. 3(d). Naturally, these models disagree among each other on the location of the higher plateaus (with $S^{\text{tot}}\geq 2$) but the latter are not probed by the experiment. Conversely, the discrepancy in Fig. 1 appearing for $H\gtrsim 50$ T between the experimental magnetization data and the best theoretical fit is not affected by the location of the $S^{\text{tot}}\geq 2$ plateaus. In our opinion, this discrepancy may originate from deficiencies in the experimental data when the magnetic field approaches its highest value, although we admit not to have a clear explanation for this at the present stage.

Finally, our theoretical model will have to acknowledge the fact that the 18-site cluster is not isolated but rather surrounded by similar clusters, which will lead to corrections to the magnetic field seen by our cluster: $H_{\text{mic}}=H_{\text{applied}}+H_{\text{corr}}$. In a mean-field approach, these corrections will weaken the applied field proportionally to the magnetization of the surrounding clusters, $H_{\text{corr}}=-\alpha M$. At the simplest level, we can use the proportionality constant α, along with the absolute value of the nearest-neighbor coupling J (i.e., expressed in Kelvin) as fit parameters for the theoretical magnetization curves to match experiment. Fixing the theoretical temperature at the experimental 1.7 K and shifting the theoretical magnetization curves by 0.011 μ_B/V^{4+} in order to account for the $S=\frac{1}{2}$ impurities not present in the models, the best agreement with experiment is obtained for the parameters listed in Table I. The theoretical curve shown in Fig. 1 corresponds to the Heisenberg ladder shown in Fig. 3(b), with $J_{\text{rung}}=1.3$ J, and to the parameter set listed in Table I.

C. Electron spin resonance results

The g-factor values mentioned at the end of the experimental section, which were deduced from X-band ESR measurements at room temperature on a single crystal, were also checked at lower temperatures at higher frequencies on powder samples. As an example, the ESR transmission data corresponding to $f=344$ GHz and obtained on a powder sample of η-$\text{Na}_{1.286}\text{V}_2\text{O}_5$ are shown in Fig. 4. These spectra are typical powder spectra for which the magnetic ion has an axial symmetry. A fit to these powder spectra using Eq. (1) (after Ibers and Swalen[10]) allows us to determine the absorbed intensity, A, and the values of the g factor for both field orientations, $g_{\parallel}$ and $g_{\perp}$.

$$I(H) \propto -\int_{H\parallel}^{H\perp} \frac{(1+H_{\parallel}^{-2}H'^2)dH'}{[(H-H')^2+b^2]H'^2(H_{\perp}^2-H'^2)^{1/2}} \qquad (1)$$

Indeed, Eq. (1) gives the appropriate line shape for a polycrystalline substance with axial symmetry and where each individual crystallite is assumed to have a Lorentzian line shape for which b would be the half width at half maximum and H' would be the resonance field.[10]

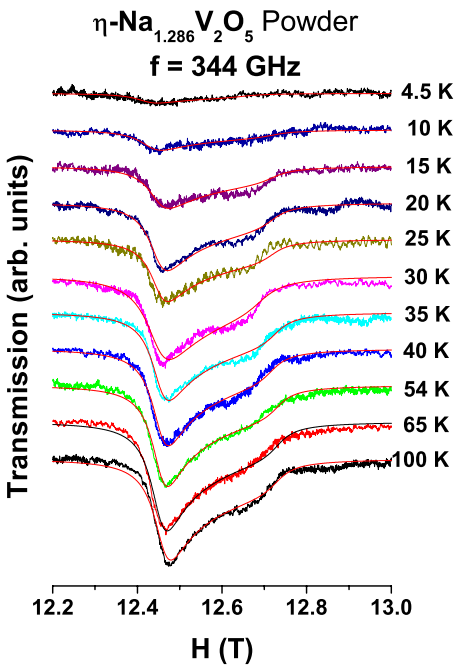

FIG. 4. (Color online) ESR spectra showing the transmitted intensity through a powder sample of η-$\text{Na}_{1.286}\text{V}_2\text{O}_5$ at a frequency of 344 GHz and at temperatures below 100 K. The continuous lines are fits to the spectra using Eq. (1) (see text for details).

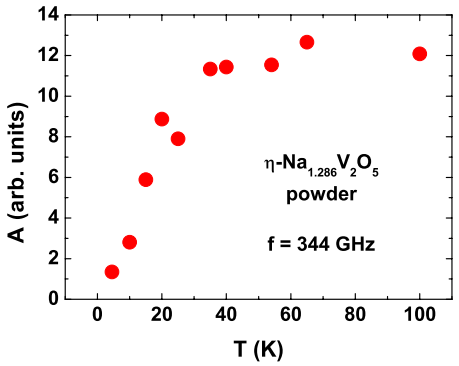

FIG. 5. (Color online) Temperature dependence of the absorption intensity, A, of a powder sample of η-$Na_{1.286}V_2O_5$ at a frequency of 344 GHz as deduced from the fits to the spectra of Fig. 4.

The temperature dependence of the absorbed intensity, A, is shown in Fig. 5, whereas that of the g factor is shown in Fig. 6.

Figure 6 confirms that, at 100 K, the g-factor values ($g_\perp = 1.931$ and $g_\parallel = 1.972$) are quite similar to the room-temperature values deduced from X-band measurements on a single crystal, and which we mentioned above. Besides, this figure shows that, apart from a slight variation at low temperature, which is due to the molecular field becoming effective, there is hardly any temperature dependence of the g factor.

Having verified the g-factor values in both field orientations on powder samples, we have then performed high-frequency (high-field) ESR measurements on single crystals of η-$Na_{1.286}V_2O_5$ in the configuration where H is perpendicular to the (x,z) plane of the structure.

We have performed these measurements at various high-frequency values ($f = 344$, 738, and 980 GHz). The first outcome of these measurements is that, to within the experimental error, the $g_\perp$ value is frequency independent.

We now present in Fig. 7 a series of spectra taken at temperatures below 40 K, for $f = 980$ GHz. [The signal appearing just below 35 T corresponds to the diphenylpicrylhydrazile (DPPH) marker.] The temperature dependence of the absorbed intensity deduced from these spectra is plotted in Fig. 8, where a comparison is made, in the same temperature range, with the intensity data measured in the X band (where $f = 9.6$ GHz). This comparison is informative as regards the ground state of the system, since the high-field value (~36.3 T), at which resonance occurs when $f = 980$ GHz, is just above the $H_c \simeq 30$ T value at which the closure of the gap takes place (see Fig. 1). Let us mention, by the way, that the X-band data shown in the left-hand panel of Fig. 8 imply a value of approximately 36 K for the gap, Δ, in accordance with our previously published estimates.[5,7]

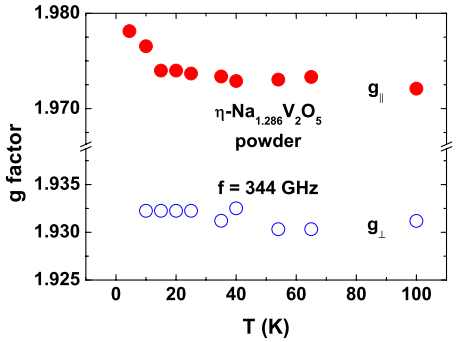

FIG. 6. (Color online) Temperature dependence of the g factor of a powder sample of η-$Na_{1.286}V_2O_5$, for both field orientations, H parallel and H perpendicular to the (x,z) plane of the structure, as deduced from the fits to the spectra of Fig. 4.

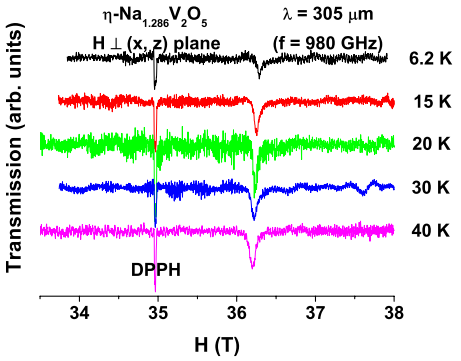

FIG. 7. (Color online) ESR spectra showing the transmitted intensity through a single crystal of η-$Na_{1.286}V_2O_5$ at a frequency of 980 GHz, in the configuration where H is perpendicular to the (x,z) plane and at temperatures below 40 K.

A close examination of the data plotted in Fig. 8 indicates that the ratio $A_{(40\ K)}/A_{(6\ K)}$ is ~215 when $f = 9.6$ GHz, whereas it is ~2.7 when $f = 980$ GHz. Knowing that the allowed transitions in ESR are only those that satisfy $\Delta S = 0$ and $\Delta S_z = \pm 1$, the measured ESR intensity is therefore proportional to the difference in population between states satisfying these conditions. ESR transitions will therefore occur mainly in the $S = 1$ triplet states (represented schematically in the inset of Fig. 1), although transitions within higher multiplet states will also occur at the same frequency. The important decrease in the $A_{(40\ K)}/A_{(6\ K)}$ ratio when $f = 980$ GHz as

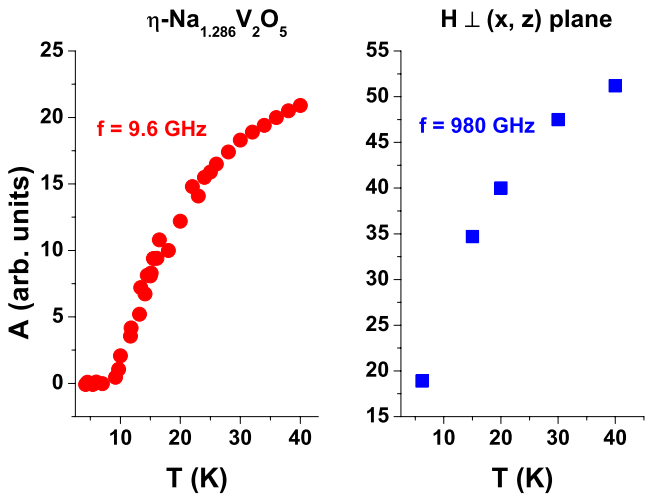

FIG. 8. (Color online) Temperature dependence of the absorption intensity, A, of a single crystal of η-$Na_{1.286}V_2O_5$ at a frequency of 980 GHz (squares) as deduced from the spectra of Fig. 7, as well as at a frequency of 9.6 GHz (circles).

compared with its value when $f=9.6$ GHz is therefore a clear indication that, at the high-field value (~36.3 T) corresponding to $f=980$ GHz, the lowest state of the triplet is much more populated at low temperature than what it is at the field value of 0.36 T (corresponding to $f=9.6$ GHz). This result is therefore a clear indication that, at 36.3 T, the lowest state of the triplet has already become the ground state of the system.

Having verified this, we have then decided to check whether or not there is an anticrossing at the critical-field value, H_c, where the change in the ground state takes place. In fact, anticrossing would occur if there is some mixing between the singlet level and the lowest level of the triplet, due, for instance, to a staggered g tensor or to the concomitant presence of a Dzyaloshinskii-Moriya interaction. If that were the case, then ESR transitions between these lowest levels, which are normally forbidden, would be allowed because of the mixing between the orbital wave functions associated with these states. We have therefore used a relatively low-frequency value, $f=96$ GHz, and tried to monitor the eventual existence at high field of ESR transitions corresponding to this frequency. Such low-frequency high-field transitions, if they became allowed, would occur at $(H_c-3.55)$ T and at $(H_c+3.55)$ T for this particular frequency. Our measurements, performed at temperatures down to 4.2 K, did not show any transition at all at these field values. The absence of such transitions constitutes, therefore, a clear indication that there is no anticrossing at H_c, it also means the absence of any appreciable Dzyaloshinskii-Moriya interaction in this compound.

IV. CONCLUSION

The aim of this work was basically twofold: it was necessary, on the one hand, to precise the value of the gap, Δ, in the magnetic excitation spectrum of η-$Na_{1.286}V_2O_5$ and, on the other hand, to check whether this compound may be regarded as a finite-size system. The high-field measurements, which we performed on this compound, coupled with a theoretical treatment of the high-field magnetization, allow us: (i) to confirm that the value of Δ is around 39 K, quite close to that which we had estimated from magnetic susceptibility and X-band ESR measurements;[5,7] (ii) to state that the magnetization data can be reproduced by several microscopic models of 18-spin $\frac{1}{2}$ clusters with the common feature that they should not be restricted to nearest-neighbor couplings. Additional couplings, such as that in a 9×2 spin ladder, or frustrating couplings, have to be introduced. But the magnetization alone is not sufficient to define the microscopic model uniquely.

Concerning whether or not this compound may be regarded as a finite-size system, we may state the following: first of all, the values of the coupling constants obtained in Table I are quite high, implying that, in this system, the AF interactions involved are quite strong. This is also the case in the high-temperature phase of this compound, since the high-temperature susceptibility data of Ref. 4 imply an AF temperature of −265 K. However, despite these strong AF interactions, the correction, H_{corr}, to the magnetic field felt by a single 18-spin unit, and which is due to the other clusters surrounding it, is only of the order of 5 T or less (cf. Table I). This constitutes a first indication that each 18-spin unit may be regarded as being relatively isolated from the other units surrounding it. A second important point is the magnetization step occurring at one ninth of the saturation magnetization: this is in perfect agreement with what would be expected in the case of isolated 18-spin units. For both of the above reasons, we deduce that η-$Na_{1.286}V_2O_5$ may be regarded as a finite-size system despite the strong AF interactions involved.

Another important conclusion of this work is that the high-field ESR study allows us also to rule out the presence of any appreciable Dzyaloshinskii-Moriya interaction in this system.

[1] Proceedings of the Seventh International Symposium on Research in High Magnetic Fields (RHMF 2003), Toulouse, France, 2003, edited by G. L. J. A. Rikken, O. Portugall, and J. Vanacken, (Elsevier, Amsterdam), [Physica B **346-347**, (2004)].
[2] Proceedings of the 17th International Conference on Magnetism (ICM 2006) Kyoto, Japan, 2006, edited by H. Harima, H. Kawamura, Y. Kitaoka, H. Kohno, K. Miyake, Y. Suzuki, H. Sakakima, and G.-q. Zheng (Elsevier, Amsterdam), [J. Magn. Magn. Mater. **310**, (2007)].
[3] P. Millet, J.-Y. Henry, and J. Galy, Acta Crystallogr., Sect. C: Cryst. Struct. Commun. **55**, 276 (1999).
[4] M. Isobe, Y. Ueda, Y. Oka, and T. Yao, J. Solid State Chem. **145**, 361 (1999).
[5] F. Duc, P. Millet, S. Ravy, A. Thiollet, F. Chabre, A. M. Ghorayeb, F. Mila, and A. Stepanov, Phys. Rev. B **69**, 094102 (2004).
[6] M.-H. Whangbo and H.-J. Koo, Solid State Commun. **115**, 115 (2000).
[7] F. Chabre, A. M. Ghorayeb, P. Millet, V. A. Pashchenko, and A. Stepanov, Phys. Rev. B **72**, 012415 (2005).
[8] J. Choukroun, V. A. Pashchenko, Y. Ksari, J. Y. Henry, F. Mila, P. Millet, P. Monod, A. Stepanov, J. Dumas, and R. Buder, Eur. Phys. J. B **14**, 655 (2000).
[9] V. A. Pashchenko, A. Sulpice, F. Mila, P. Millet, A. Stepanov, and P. Wyder, Eur. Phys. J. B **21**, 473 (2001).
[10] J. A. Ibers and J. D. Swalen, Phys. Rev. **127**, 1914 (1962).